Pyramidal Wavefront Sensor Demonstrator at INO

Olivier Martin*[a], Jean-Pierre Véran [b], Geneviève Anctil[a], Pascal Bourqui[a], François Châteauneuf[a], Jonny Gauvin[a], Philippe Goyette[a], François Lagacé[a], Simon Turbide[a], Min Wang[a], [a]Institut National d'Optique, 2740 rue Einstein, Québec, QC, G1P 4S4 Canada; [b]Herzberg Institute of Astrophysics, NRC-CNRC, 5071 West Saanich Road, Victoria, BC V9E 2E7, Canada

ABSTRACT

Wavefront sensing is one of the key elements of an Adaptive Optics System. Although Shack-Hartmann WFS are the most commonly used whether for astronomical or biomedical applications, the high-sensitivity and large dynamic-range of the Pyramid-WFS (P-WFS) technology is promising and needs to be further investigated for proper justification in future Extremely Large Telescopes (ELT) applications. At INO, center for applied research in optics and technology transfer in Quebec City, Canada, we have recently set to develop a Pyramid wavefront sensor (P-WFS), an option for which no other research group in Canada had any experience. A first version had been built and tested in 2013 in collaboration with NRC-HIA Victoria. Here we present a second iteration of demonstrator with an extended spectral range, fast modulation capability and low-noise, fast-acquisition EMCCD sensor. The system has been designed with compactness and robustness in mind to allow on-sky testing at Mont Mégantic facility, in parallel with a Shack-Hartmann sensor so as to compare both options.

Keywords: Adaptive optics, Wavefront sensor, Pyramid, PWFS, Demonstrator, INO

1. INTRODUCTION

The Pyramid wavefront sensor (P-WFS) is an evolution of the standard Foucault knife-edge test to allow a quantitative estimation of the spatial derivative of the wavefront distortion. It was first proposed by Ragazzoni[1] in 1996 and since then successfully implemented on large telescopes AO systems like the one at LBT[2].

In comparison with the Shack-Hartmann wavefront sensor, the P-WFS claims better sensitivity[3], greater adaptation to the correcting wavelength, seeing conditions and brightness of the source thanks to the possibility to change the spatial sampling and gain during operation by binning on the detector and variation of the amplitude of modulation. Unlike the SH-WFS, which uses small-aperture micro-lenses to sample the telescope pupil, a P-WFS is only limited by diffraction effects introduced by the whole telescope aperture. It offers more range in limiting magnitude because it is less affected by aliasing at the bright end and it is more sensitive at the faint end than a SH-WFS. The principle of operation of the P_WFS will be described in Section 2.

On the other hand, the need for dynamic modulation can be a disadvantage because it requires a moving component at high frequency inside the instrument. Also the very nature of the pyramid prism can introduce chromatic aberrations and limit the wavelength spectral range of the WFS. In Section 3 we present the preliminary phase set-up built at INO[4] in order to gain experience with the concept of P-WFS. Results of the first phase will also be briefly recalled. The second iteration (still ongoing at the time of redaction of this paper) with an extended spectral range, fast modulation capability and low-noise, fast-acquisition EMCCD sensor will be discussed in Section 4.

2. PRINCIPLE OF OPERATION

The principle of operation is shown in Figure 1. Four images of the entrance pupil – itself conjugate to the telescope pupil – are produced by a pyramid-shaped prism onto the detector by means of a telecentric lens system. Modulation of the pupil by means of a tip-tilt mirror is key to obtaining the quantitative information on the wavefront distortion and telecentricity of the system ensures that pixels remain co-registered in the four pupil images in the detector plane as the pupil is modulated.

*olivier.martin@ino.com; phone 1 418 657-7006 ext. 2710; fax 1 418 657-7009; www.ino.com

Adaptive Optics Systems IV, edited by Enrico Marchetti, Laird M. Close, Jean-Pierre Véran, Proc. of SPIE Vol. 9148, 91485X · © 2014 SPIE
CCC code: 0277-786X/14/$18 · doi: 10.1117/12.2056893

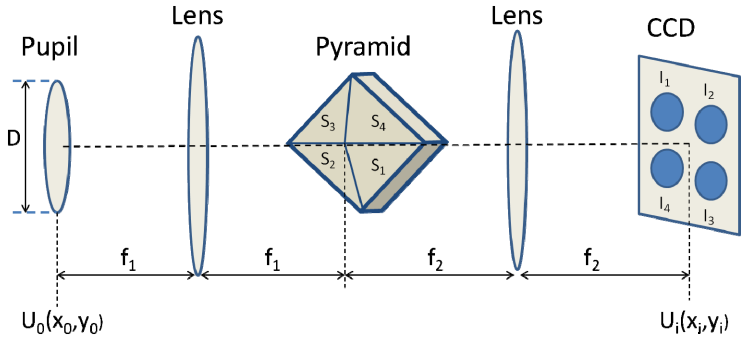

Figure 1. Schematic representation of the P-WFS.

The P-WFS signals are defined as a combination of the four pupil images averaged over the modulation period:

$$S_x(x,y) = \langle I_1(x,y)\rangle + \langle I_4(x,y)\rangle - \langle I_2(x,y)\rangle - \langle I_3(x,y)\rangle$$
$$S_y(x,y) = \langle I_1(x,y)\rangle + \langle I_2(x,y)\rangle - \langle I_3(x,y)\rangle - \langle I_4(x,y)\rangle \quad (1)$$

where the coordinates (x,y) refer to co-registered pixels in the four pupil images. In the limit of small aberrations the P-WFS signals can be decomposed in a sum of interaction matrices, themselves functions of Zernike polynomials. Wavefront reconstruction is then derived from the response matrix combined from the measured *x* and *y* signals.

3. P-WFS DEVELOPMENTS AT INO: PRELIMINARY PHASE

Figure 2 shows a view of the overall test-bench for P-WFS developments at INO[4]. The system was optimized for a single wavelength and used as many components off-the-shelf as possible. It consisted of a waveform generator and a separate breadboard containing the modulation mirror, pyramid and associated optics, and CCD camera.

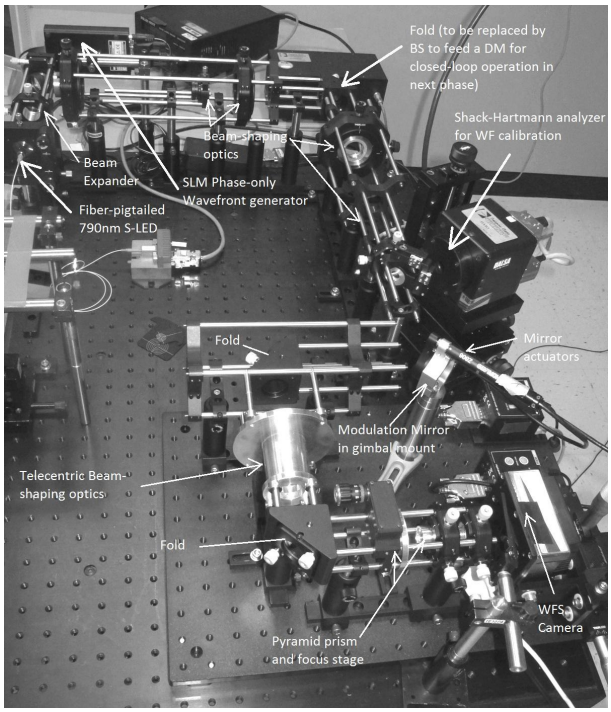

Figure 2. First iteration P-WFS test-bench (single wavelength).

Waveform generation involved a 790 nm wavelength super-luminescent LED with 30nm FWHM, a phase-only LCD spatial phase modulator optimized for visible light and formatting optics. A commercial Shack-Hartmann provided monitoring of the wavefront and helped with calibration of the beam train.

Pupil size of about 5 mm at the modulation mirror and f/45 lens produced an 85µm spot at the tip of the pyramid compatible with the prism geometry. Due to the difficulty to manufacture a prism with very shallow angles (θ=3.379^o between facets), the actual shape of the pyramid tip was slightly rectangular, 50µm by 30µm as seen on the picture in Figure 3.

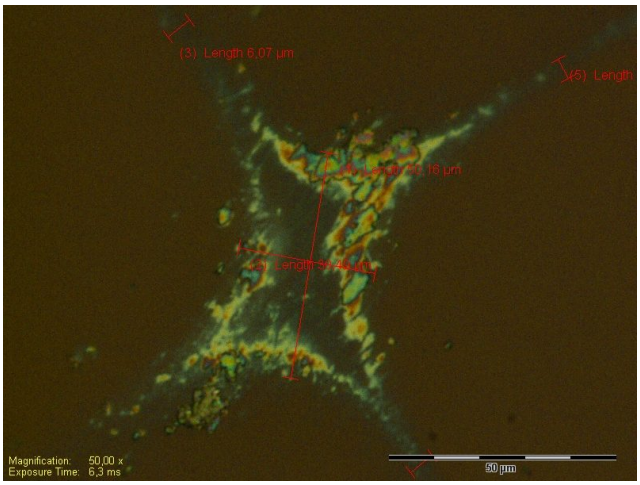

Figure 3. Tip of the pyramid as seen under a microscope.

In spite of limitations of the system due to the lack of accuracy and repeatability of the modulation movements from the commercial mirror actuators and inherent vibration and noise of the CCD camera that compelled to average data points over 30 images (thus limiting the possibility of closed loop operation), a good agreement was observed between simulations and actual data in terms of reconstruction errors. The P-WFS appeared to have better reconstruction error than the Shack-Hartmann, at least for the no-modulation case, as seen in Figure 4.

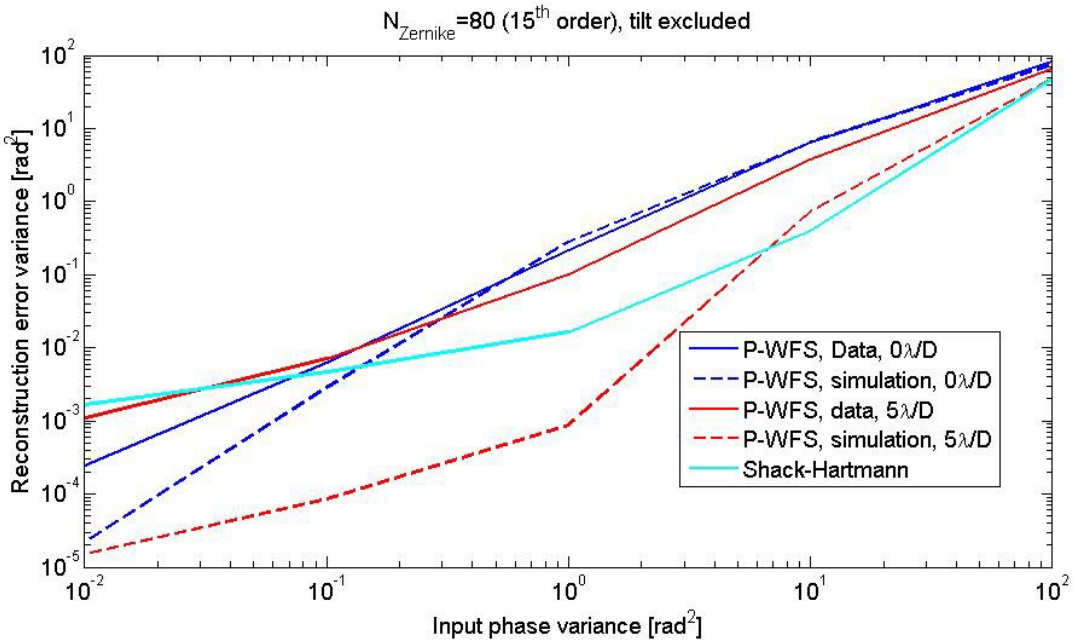

Figure 4. Reconstruction error variance of the P-WFS as a function of input phase variance based on 80 Zernike coefficients.30 images (at 60 fps) co-added for each point. Comparison with the simulated Shack-Hartmann performance.

Based on encouraging performance of the system built around low cost components, we decided to work on further improvements of the system in terms of spectral pass-band, speed and noise.

After the first P-WFS set-up was built and tested in house at INO, the system was sent to our collaborators at HIA Victoria. It was integrated there in the AO development test-bench with a fast piezo tip-tilt actuator to replace the slower modulation mirror and a MEMS deformable mirror to generate high-order Fourier aberrations. Results are presented in another paper in these proceedings[5].

4. P-WFS DEVELOPMENTS AT INO: SECONDARY PHASE

4.1 Optical design

Improvement of the system is linked to a number of upgrades:

- Extended spectral range in the red to near-infrared band, at least 600 to 800nm in order to approach a realistic situation with a natural guide star.
- Fast piezo tip-tilt actuator to allow modulation close to 500 Hz.
- High-sensitivity, low-noise camera to improve the overall signal-to-noise ratio.
- Rugged and stable mechanical interface of the P-WFS module to allow on-sky tests on a professional telescope. Another group at Laval University in Québec is developing a new AO test box for Mont Mégantic Observatory and will present the design in these proceedings[6]. A joint observing campaign is currently planned in order to compare side-by-side performance of Shack-Hartmann and P-WFS.
- Implementation of a Deformable Mirror (DM) in the beam train for closed-loop operation.

The overall layout of the test bench remains unchanged as seen in Figure 5 but all optics on the beam injection and calibration side have been replaced to ensure at least λ /10 to λ /15 P-V (or at least λ/20 RMS) wavefront error in input of the P-WFS system, at the Tip-Tilt Mirror (TTM).

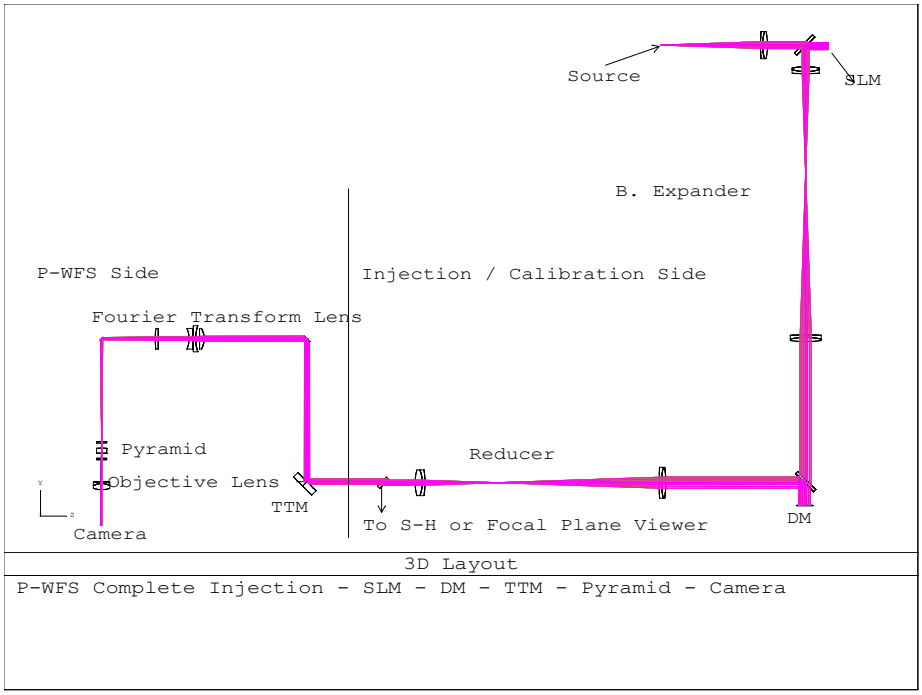

Figure 5. Optical layout of the pyramid wavefront sensor test-bench.

All beam shaping optics are off-the-shelf components optimized for 650-1050 nm. A fiber-pigtailed Halogen-Tungsten white light source is used in injection. Combinations of long-pass and short-pass colored filtered help limit the spectral range in 100 nm or 200 nm bands between 600nm and 900 nm in order to verify the chromatic effects on the P-WFS operation and mitigate the effects if necessary

The set-up includes a phase-only SLM optimized for 420-700nm and a 69-actuator face-sheet Deformable Mirror. The DM can be left at rest when the SLM is used as a turbulence generator for open-loop characterization of the P-WFS or as a proper DM to close the AO loop. The DM can also be used as a turbulence generator if the SLM is proved not to be suited to the large spectral range, in which case the beam-splitter in front of the SLM will be replaced by a fold mirror. DM and Tip-Tilt Mirror are conjugate so that the DM pupil is also conjugate to the four pupils produced by the pyramid on the sensor camera.

The commercial Shack-Hartmann sensor between the beam reducer and the TTM can help calibrate static errors (wavefront aberrations introduced by components and alignment defects). On the other hand, aberrations introduced between the modulation mirror and camera cannot be measured or calibrated by the control Shack-Hartmann so they can be considered as "non-common path errors" and have to be limited as much as possible by design and careful alignment.

Modulation is provided by a piezo tip-tilt platform from PI with a closed-loop travel range of 5 mrad in θX and θY and 4 kHz resonant frequency. Sine movements are controlled from a PC digital-to-analog conversion card. We aim at reaching 400Hz to 500Hz modulation frequency while synchronizing camera acquisition trigger. Control software has been developed and will be validated as the system is implemented.

The original Fourier transform lens between the TTM and pyramid was re-used due to its good optical quality over an extended spectral range and because the very large f/ number provided a large depth of field. On the other hand the magnification lens between pyramid and camera required some optimization to fit the new camera. Magnification of the four sub-pupils has to be set so that each sub-pupil occupies a given number of pixels on the CCD matrix.

The camera has been upgraded to a back-illuminated Electron Multiplying CCD from Nüvü, model HNü 512, with stable thermoelectric temperature control to -90°C. Pixels are 16 µm on a side and maximum frame rate when unbinned is close to 200 fps, whereas we would like to trigger frames as fast as possible in order to be able to close the AO loop on a star. To achieve ~500 fps it will be necessary to use 2x2 binning and Regions of Interest on the camera. One would be tempted to use a long focal length lens to spread out the images sub-pupils on the as large an area as possible but the effect of chromatic dispersion introduced by the pyramid also need to be taken into account. Because of the differential refraction index within the pyramid over the wavelength range, the sub-pupils will be offset. For the AO loop to be closed, the maximum DM to WFS registration error (including pupil offsets and error of pupil position, induced by the uncertainty on the position of pupil centroid) should not exceed 1/10 of the equivalent pitch between DM actuators. At INO the 69-actuator ALPAO DM has 9 actuators on a side, for a 10.5mm pupil, whereas the set-up developed by Laval University for Mt-Megantic telescope is a 97-actuator DM with the same pitch. P-WFS sub-pupils should then be at least 10 pixels wide or a multiple of 10, with total registration error of less than 0.1pixel.

Entrance pupil diameter is scaled by the magnification between first and second lens and sub-pupil separation on the sensor is proportional to the focal length of the second lens:

$$D_{subpupil} = D_{TTM}\ f_2/f_1 \qquad (2)$$

$$\Delta_{interpupil} = 2f_2(n_0-1)\tan\alpha \qquad (3)$$

where α is the edge-angle of the pyramid, about 2.39°, n_0 is the pyramid refractive index and D_{TTM} is the pupil diameter on the tip-tilt mirror. In fact, the pyramid is not perfectly symmetric and four angles can be defined as seen in Figure 6, so the offset between sub-pupils would be as shown in Figure 7:

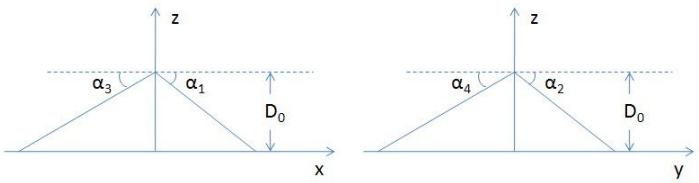

Figure 6. Profile views of the pyramid in the Z-X and Z-Y planes.

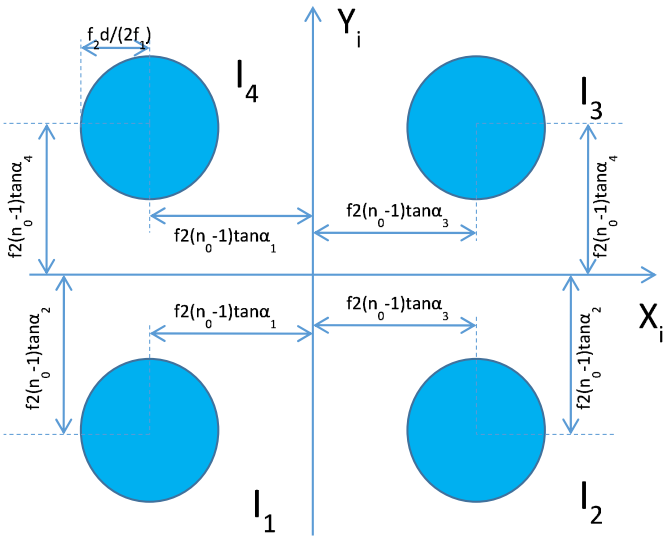

Figure 7. P-WFS system generates four images of the pupil plane; position of each image is function of the pyramid angles.

As a first approximation, all angles are equal and table 1 shows the results as f_2 is varied:

Table 1. Sub-pupil size, distance between sub-pupils, absolute pupil shift over the wavelength range and relative shift after camera pixel binning as a function magnification lens focal length.

f_2 (mm)	30	35	40	50
$D_{subpupil}$	560µm (35 camera pixels)	653 µm (40.8 pixels)	747 µm (46.7 pixels)	900 µm (56.25 pix)
$\Delta_{interpupil}$	1152 µm (72 pixels)	1343 µm (83.9 pixels)	1536 µm (96 pixels)	1918 µm (119.9 pix)
Chromatic shift (λ 600 to 800nm / 600 to 900nm)	4.2 µm or 5.6 µm	4.9 µm or 6.3 µm	6.3 µm or 7.8 µm	8.5 µm or 10.6 µm
Binning possible?	No or 2x2 (for 17.5 pixels over 9 or 11 DM actuators)	2x2 or 4x4 (for 10.2 pixels over DM pupil)	2x2 or 4x4 (for 11.67 pix over DM pupil)	2x2 or 4x4 (14.06 pix over DM pupil)
Relative shift after binning	4.2 or 5.6/16≈0.26 or 0.35pix (no binning) 0.13 or 0.18 (2x2 binning)	4.9 or 6.3/32≈0.15 or 0.20pix (2x2 binning) 0.08 or 0.1 (4x4 binning)	0.20 or 0.24 pix (2x2 bin) 0.10 or 0.12 pix (4x4 bin)	0.27 or 0.33 pix (2x2 binning) 0.14 or 0.17 pix (4x4 binning)

As can be seen, 35mm is the optimal focal length for the imaging lens, still allowing 4x4 binning on the camera and consequently 400 fps acquisition or faster if ROI are introduced to reduce transfer time. There is almost one-to-one matching between DM actuators and sub-pupil pixels, while approaching the 0.1 pixel maximum admissible error.

As a conclusion of the optical redesign study, it might not be possible to achieve a very large spectral bandwidth using a single fused silica pyramid. The limiting factor is not the optical quality of the beam formatting lenses but by the size of the camera pixels and the chromatic dispersion of the pyramid itself (which cannot be compensated by a single wedge, as the 4 images formed by the faces are diverging from the common optical axis). We will have to experiment by using colored filters in order to determine the optimal spectral range that allows closing the loop.

4.2 Mechanical design

Originally the P-WFS and its associated test bench had been built using only laboratory opto-mechanical components, suitable for use in a static environment but not onboard a telescope. We are redesigning the P-WFS with custom supports for the TTM and camera in a way that still allows laboratory tests and also provides sufficient stability when the system will be attached to the mechanical interface on Mont-Mégantic telescope. Figure 8 shows the focal plane AO test box with the P-WFS system attached; Figure 9 gives a better view of the P-WFS components.

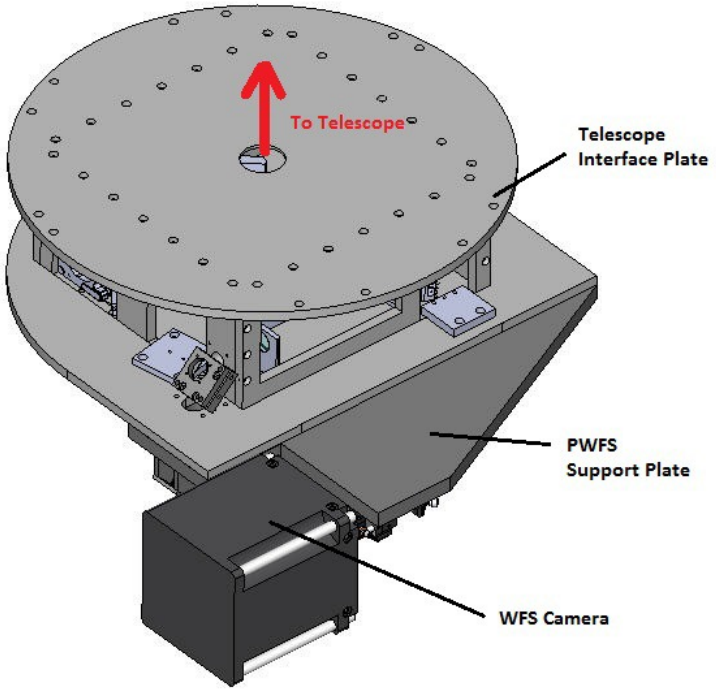

Figure 8. Schematic view of the AO test box with the P-WFS attached below.

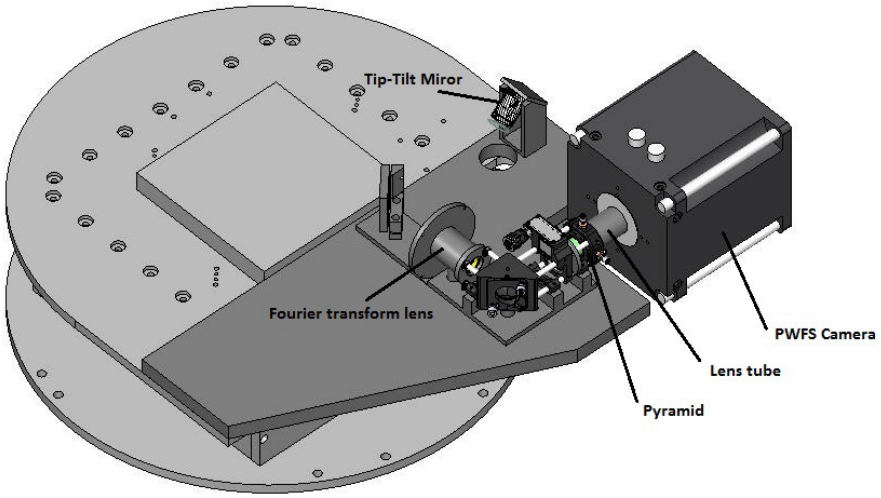

Figure 9. Bottom view of the Mont-Mégantic adaptive optics test box with all P-WFS components.

5. CONCLUSION

Development work is ongoing at INO towards the construction of a second Pyramid Wavefront Sensor demonstrator that will be validated in house as a complete AO system. The limits of applicability of a single pyramid prism for extended wavelength range wavefront sensing will be measured. We hope to confirm the results shown by the first demonstrator regarding superior performance of the P-WFS over the Shack-Hartmann in the low turbulence regime while improving the performance in terms of dynamic range and sensitivity. Non-linear reconstruction algorithms which had been developed in parallel to this project will be implemented to help extend sensitivity in conditions of high input variance. Improved mechanical interface of the wavefront sensor stage will allow to fit the system to an AO test box developed by another group for Mont-Mégantic Observatory. A joint observing campaign will focus on comparing near-simultaneous on-sky performance of Shack-Hartmann and Pyramid wavefront sensors.

Experience acquired by INO will be invaluable in the perspective of offering technological solutions to our partners in the domain of wavefront sensing and adaptive optics in general.

REFERENCES

[1] Ragazzoni, R., J. Mod. Opt. **43**, 289, (1996).

[2] Esposito, S. *et al*., "Natural guide star adaptive optics system at LBT: FLAO commissioning and science operation status," Proc. SPIE 8447, 84470U (2010).

[3] Esposito, S. and Riccardi, A., "Pyramid Wavefront Sensor behavior in partial correction Adaptive Optics systems," A&A 369, L9-L12 (2001).

[4] Turbide, S. *et al*., "Development of a pyramidal wavefront sensor test-bench at INO," in [Adaptive Optics for Extremely Large Telescopes III], AO4ELT3 Conference Proceedings (2013).

[5] Rosensteiner, M and Véran, J-P., "Testing the analytical model of the pyramid wavefront sensor with high-order aberrations on the optical bench," Proc. SPIE 9148, paper 9148-196 (these proceedings).

[6] Brousseau, D. *et al*., "The focal plane adaptive optics test box of the Observatoire du Mont-Mégantic," Proc. SPIE 9148, paper 9148-211 (these proceedings).